HHS Public Access

Author manuscript

J Bone Miner Res. Author manuscript; available in PMC 2015 October 01.

Published in final edited form as:

J Bone Miner Res. 2015 October ; 30(10): 1822–1830. doi:10.1002/jbmr.2514.

High-bone-mass causing mutant LRP5 receptors are resistant to endogenous inhibitors *in vivo*†

Paul J. Niziolek[1,2], **Bryan T. MacDonald**[3,4], **Rajendra Kedlaya**[1], **Minjie Zhang**[5,6], **Teresita Bellido**[1], **Xi He**[3,4], **Matthew L. Warman**[5,6], and **Alexander G. Robling**[1,7,8,*]

[1]Department of Anatomy & Cell Biology, Indiana University School of Medicine, Indianapolis, IN, USA

[2]Weldon School of Biomedical Engineering, Purdue University, West Lafayette, IN, USA

[3]The F.M. Kirby Neurobiology Center, Boston Children's Hospital, Boston, MA, USA

[4]Department of Neurology, Harvard Medical School, Boston, MA USA

[5]Howard Hughes Medical Institute, Boston Children's Hospital, Boston, MA, USA

[6]Departments of Orthopaedic Surgery and Genetics, Harvard Medical School, Boston, MA, USA

[7]Department of Biomedical Engineering, Indiana University–Purdue University at Indianapolis (IUPUI), Indianapolis, IN, USA

[8]Richard L. Roudebush VA Medical Center, Indianapolis, IN USA

Abstract

Certain missense mutations affecting LRP5 cause high bone mass (HBM) in humans. Based on *in vitro* evidence, HBM LRP5 receptors are thought to exert their effects by providing resistance to binding/inhibition of secreted LRP5 inhibitors such as sclerostin (SOST) and Dickkopf homolog-1 (DKK1). We previously reported the creation of two *Lrp5* HBM knock-in mouse models, in which the human p.A214V or p.G171V missense mutations were knocked into the endogenous *Lrp5* locus. To determine whether HBM knock-in mice are resistant to SOST- or DKK1-induced osteopenia, we bred *Lrp5* HBM mice with transgenic mice that overexpress human SOST in osteocytes (^{8kb}*Dmp1-SOST*) or mouse DKK1 in osteoblasts and osteocytes ($^{2.3kb}$*Col1a1-Dkk1*). We observed that the ^{8kb}*Dmp1-SOST* transgene significantly lowered whole body BMD, BMC, femoral and vertebral BV/TV, and periosteal BFR in wild-type mice but not in mice with *Lrp5* p.G171V and p.A214V alleles. The $^{2.3kb}$*Col1a1-Dkk1* transgene significantly lowered whole body BMD, BMC, and vertebral BV/TV in wild-type mice and affected p.A214V mice more than p.G171V mice. These *in vivo* data support *in vitro* studies regarding the mechanism of HBM-

---

†This article has been accepted for publication and undergone full peer review but has not been through the copyediting, typesetting, pagination and proofreading process, which may lead to differences between this version and the Version of Record. Please cite this article as doi: [10.1002/jbmr.2514]

Corresponding Author: Alexander G. Robling, Ph.D., Department of Anatomy & Cell Biology, Indiana University School of Medicine, 635 Barnhill Dr., MS 5035, Indianapolis, IN 46202, Tel: (317) 274-7489, Fax: (317) 278-2040, arobling@iupui.edu.

Additional Supporting Information may be found in the online version of this article.

Disclosure Statement: The authors have nothing to disclose.

causing mutations, and imply that HBM LRP5 receptors differ in their relative sensitivity to inhibition by SOST and DKK1.

Keywords

WNT; LRP5; high bone mass (HBM); SOST; sclerostin; DKK1; G171V; A214V; osteoporosis

Introduction

The recent discovery and elucidation of the importance of WNT signaling in bone metabolism has presented new opportunities for the development of treatment options for osteoporosis, fracture healing, and other skeletal disorders [(1)]. The crucial role of WNT signaling in normal, healthy bone tissue was demonstrated initially when the genetic cause of the Osteoporosis Pseudoglioma syndrome (OPPG) was identified. This autosomal recessive disease characterized by low bone mass and blindness is caused by loss-of-function mutations affecting the WNT co-receptor LDL-Receptor-Related Protein 5 (LRP5) [(2, 3)]. Investigation into the cause of high bone mass (HBM) phenotypes in humans next identified missense mutations in LRP5, suggesting that gain- and loss-of function mutations in this receptor have substantial and opposing effects on bone mass and strength. A similar role in modulating bone mass has been demonstrated for LRP6, a closely related paralog of LRP5, underscoring the importance of WNT signaling in general for attainment of peak bone mass [(4–7)].

That missense mutations in LRP5 produce an HBM phenotype prompted investigation into the mechanism by which these single amino acid changes alter the receptor's ability to transduce WNT signals. *In vitro* cell transfection experiments found that most HBM LRP5 receptors respond normally to agonistic WNT ligands, but are less inhibited by endogenous LRP5 antagonists, including Dickkopf homolog-1 (DKK1) and sclerostin (SOST) [(8–12)]. Consistent with these findings, LRP5 HBM mutations cluster in the first β-propeller domain surrounding the structurally mapped SOST "NxI" motif binding pocket [(13)]. Similar to SOST, DKK1 also has an "NxI" motif that binds to the first β-propeller [(13, 14)], but DKK1 also has an additional domain that binds to the third β-propeller of LRP5/6 [(15–17)]. It is unclear which LRP5/6 binding domain in DKK1 is responsible for the majority of its endogenous inhibitory function [(18)]. A second mechanism has been proposed for at least one HBM LRP5 mutation, p.G171V, which implicates impaired trafficking to the cell membrane but retention of the receptor's WNT signal transduction ability. This second mechanism implies that resistance to SOST and DKK1 is due to less LRP5 reaching the cell surface, rather than to reduced affinity between LRP5 and its extracellular inhibitors [(19)]. A limitation for all *in vitro* studies is that they have been performed in cells that overexpress LRP5.

In the present communication, we assess the *in vivo* actions of SOST and DKK1 in mice that have *Lrp5* HBM-causing knock-in alleles. We explored this interaction by cross-breeding (A) transgenic mice that overexpress murine DKK1 in osteoblasts and osteocytes ($^{2.3kb}$*Col1a1-Dkk1*) with knock-in mice that harbor either the p.G171V or p.A214V

mutation in *Lrp5*; and (B) transgenic mice that overexpress human SOST in osteocytes (^{8kb}*Dmp1-SOST*) with *Lrp5* p.G171V or p.A214V knock-in mice. The $^{2.3kb}$*Col1a1-Dkk1* and ^{8kb}*Dmp1-SOST* transgenic mice exhibit an osteopenic phenotype [20, 21], whereas the *Lrp5* HBM knock-in mice exhibit a high bone mass phenotype [22].

Based on previously published *in vitro* work, we anticipated that bone in *Lrp5* HBM knock-in mice would be protected from the osteopenic effects caused by overexpression of SOST and possibly protected from the effects caused by DKK1 overexpression. Here, we report that SOST overexpression does not significantly reduce bone properties in *Lrp5* HBM mice and that DKK1 overexpression significantly affects p.A214V mice more than p.G171V mice.

Materials and Methods

Animals

All animal procedures were performed in accordance with guidelines set by the Indiana University Institutional Animal Care and Use Committee.

Mice with the *Lrp5* knock-in HBM mutations p.A214V and p.G171V have been described previously [22] as have *Lrp5* knockout mice.[23] The HBM mice were on a mixed 129S1/SvIMJ and C57Bl/6J background. $^{2.3kb}$*Col1a1-Dkk1* transgenic mice have been described previously.[20] Briefly, a 2.3kb fragment of the rat *Col1a1* promoter drives expression of mouse *Dkk1* cDNA. The $^{2.3kb}$*Col1a1-Dkk1* transgenic mice were on an FVB background. ^{8kb}*Dmp1-SOST* transgenic mice have been described previously [21]. Briefly a 12kb DNA fragment containing 8 kb of the 5′-flanking region, the first exon, the first intron, and 17 bp of exon 2 of the murine *Dmp1* gene was used to drive expression of a human *SOST* cDNA. The ^{8kb}*Dmp1-SOST* mice were on a fixed C57Bl/6J background. *Lrp5* HBM mice were crossed with ^{8kb}*Dmp1-SOST* and $^{2.3kb}$*Col1a1-Dkk1* transgenic mice for several generations to generate mice that were homozygous for the *Lrp5* alleles; i.e., $Lrp5^{+/+}$ (henceforth denoted WT), $Lrp5^{A214V/A214V}$ (henceforth denoted *Lrp5* A214V), or $Lrp5^{G171V/G171V}$ (henceforth denoted *Lrp5* G171V) and either positive or negative for the *SOST* or *Dkk1* transgene. WT mice were derived from the same litters as transgenic mice, within each *Lrp5* background. The *Lrp5*, *SOST*, and *Dkk1* alleles were identified in mice using standard PCR techniques on genomic DNA from tail clips. For each of the analyses, 8 mice per group were used unless otherwise indicated.

Dual energy x-ray absorptiometry (DEXA)

Longitudinal characterization of whole body (excluding skull) bone mineral content (BMC) and areal bone mineral density (aBMD) were measured using PIXImus2 (GE Lunar). Mice were anesthetized with isoflurane (2% @ 1.5 liters/min) and placed in a prone position with limbs outstretched. Whole-body scans were collected every 2 wks, beginning at 4.5 wks and extending to 16.5 wks of age.

Micro-computed tomography (μCT)

The right femur and 5th lumbar vertebra were extracted from euthanized mice at 17 wks of age. The bones were fixed in 10% NBF for 2 days and then stored in 70% ethanol. At the time of scanning (Skyscan 1172, Bruker, Inc., Kontich, Belgium), the femurs were suspended in a tube containing a thermoreversible gel (Pluronic® F108) to securely immobilize the bones during the scan [24]. Acquisition settings were 60 kV peak tube potential, 1000×524 camera size, 0.4° step size, 151-ms integration time, and a resolution of 10.04 microns/pixel.[25] Trabecular bone was segmented from cortical bone manually using the Skyscan software CTAn. For both SOST and DKK1overexpression studies, the analysis region for L5 contained all trabecular bone between both growth plates (excluding the primary spongiosa). For the distal femur, different analysis regions or the secondary spongiosa were implemented for each study. For the ^{8kb}*Dmp1-SOST Lrp5* HBM experiment, a region 275 slices (~2.76mm) in height was used. For the $^{2.3kb}$*Col1a1-Dkk1 Lrp5* HBM experiment, a region 225 slices (~2.26mm) in height was used. Different sections were used for the two different transgenic mouse models, based on preliminary analyses of transgenic and non-transgenic mice that identified the metaphyseal portion most affected by each transgene.

Dynamic histomorphometry

Mice received intraperitoneal injections of bone-labeling fluorochromes over the course of the study. Oxytetracycline (60 mg/kg) was injected at 5 weeks, calcein (18 mg/kg) at 8 weeks, and alizarin (20 mg/kg) at 12 weeks. Following μCT measurement, the L5 and femur were dehydrated in graded alcohols, cleared in xylene, and embedded in methylmethacrylate following standard protocols. Thick-cut sections were taken at the midshaft and ground down to ~30 μm. Unstained sections were digitally imaged on a fluorescence microscope using filter sets that provide excitation and emission for the tetracycline, calcein, and alizarin wavelengths. Digital images were imported into ImagePro Express (Media Cybernetics, Inc., Gaithersburg, MD) and the following histomorphometric measurements were recorded between the calcein and alizarin labels for the periosteal and endocortical surfaces: total perimeter (B.Pm), single label perimeter (sL.Pm), double label perimeter (dL.Pm), double label area (dL.Ar), total bone area and marrow area. The following results were calculated: mineral apposition rate (MAR = dL.Ar/dL.Pm/28 days), mineralizing surface (MS/BS = (0.5* sL.Pm + dL.Pm)/B.Pm*100), and bone formation rate (BFR/BS = MAR * MS/BS * 3.65).

Measurements of serum carboxy-terminal collagen crosslinks (CtX)

Blood samples were collected from mice at 7 wks of age, allowed to clot for 30–60 min, and then centrifuged to separate blood components. Serum was frozen at −80°C. Serum crosslinks were measured using a commercially available plate assay (IDS Ratlaps EIA) following manufacturer's instructions. Serum samples from seven mice per group were analyzed.

Three-point bending

The left femurs from the 17-wk-old euthanized mice were removed, wrapped in saline soaked gauze, and stored at −20°C. On the day of testing, the femurs were allowed to warm to room temperature for at least 2 hours. The femoral length was measured with digital calipers, then the femoral diaphysis was broken using a 3-point bending system (EnduraTEC) that recorded force and displacement [(26)]. Based on these data, the structural properties ultimate force, stiffness, and energy to ultimate force were calculated using standard equations.

Immunoblotting

Protein was extracted from femoral diaphysis cortical tubes (marrow removed) and liver from 8-wk-old *Lrp5* HBM, WT, and knockout mice. Tissue samples were homogenized in T-Per tissue protein extraction reagent (Thermo-Fisher Scientific, Waltham, MA, USA) using the FastPrep-24 Instrument (MP Biochemicals, Santa Ana, CA, USA) and then centrifuged at 10,000g for 5 minutes. The supernatant was collected and assayed for total protein using the Coomassie Plus Protein Assay kit (Pierce Biotechnology, Rockford, IL, USA). Fifteen μg aliquots of protein extract were separated by SDS-PAGE, transferred to PVDF, and probed with anti-LRP5 antibody (D5G4; Cell Signaling, Danvers, MA, USA) and anti-β-actin antibody (Sigma, St Louis, MO, USA) at a dilution of 1:1000. The blots were incubated in species-appropriate HRP-conjugated secondary antibodies and immune complexes were detected using the WesternBreeze chemiluminescence kit (Life Technologies, Grand Island, NY).

Statistical methods

Longitudinal data were analyzed by repeated measures ANOVA comparing transgenic to nontransgenic mice within a sex/*Lrp5* genotype group. All other data were compared using student's t-test for transgenic to nontransgenic mice within a sex/*Lrp5* genotype group. Significance was taken at $p < 0.05$. All data are presented as mean ±SE.

Results

I. A214V and G171V mice are resistant to the osteopenic effects of SOST overexpression

To assess the suppressive effects of SOST overexpression on bone we first evaluated the effects of the ^{8kb}*Dmp1-SOST* transgene on whole body areal bone mineral density (aBMD) and content (BMC) in *Lrp5* WT mice. Consistent with previous reports,[(21)] SOST overexpression resulted in a significant reduction in bone mass (Fig. 1 A&B; Fig S1). SOST overexpression reduced aBMD by 9% in *Lrp5* WT males (p=0.002) and by 4% in *Lrp5* WT females (p=0.063). In contrast SOST overexpression did not significantly reduce aBMD in either male or female *Lrp5* A214V mice (p=0.11 and p=0.38), respectively) or G171V mice (p=0.42 and p=0.87, respectively) (Fig. 1A&B).

We next analyzed femora from 16 wk-old *Lrp5* WT and *Lrp5* HBM mice with and without the ^{8kb}*Dmp1-SOST* transgene. SOST overexpression reduced the distal femur trabecular bone volume fraction (BV/TV) by 70% in *Lrp5* WT males (p<0.001) and by 40% in *Lrp5* WT females (p=0.02) (Fig. 1C&E). In contrast, SOST overexpression did not reduce distal

femur BV/TV by more than 15% in male or female *Lrp5* A214V or G171V mice ($p>0.05$ for all comparisons); distal femur trabecular number and trabecular spacing also differed significantly when SOST was overexpressed in *Lrp5* WT mice, but not when SOST was overexpressed in *Lrp5* A214V or G171V mice (Table S1).

Analysis of the 5th lumbar vertebra (L5) revealed that SOST overexpression reduced trabecular bone mass by ~50% in male and female *Lrp5* WT mice ($p<0.001$ for both sexes), but did not significantly reduce BV/TV in the *Lrp5* HBM mice (Fig. 1D). *Lrp5* HBM mice were not completely resistant to SOST overexpression, as assessed by examining other trabecular bone parameters (Table S1), but the effect of SOST overexpression in both *Lrp5* HBM mice was less than that observed in *Lrp5* WT mice.

Fluorochrome labels injected prior to sacrifice allowed us to measure changes in bone formation rates induced by SOST overexpression within the *Lrp5* WT and HBM backgrounds. The *SOST* transgene significantly decreased periosteal bone formation rates (BFR/BS) by 15% in male *Lrp5* WT mice ($p=0.03$) and by 22% in female *Lrp5* WT mice ($p=0.03$), but the transgene did not significantly affect BFR/BS in either *Lrp5* HBM strain (Fig. 2A&B, Table S2). The transgene had the opposite effect on the endocortical surface (Table S2). SOST overexpression had no effect on CtX values in WT or HBM mice (Fig 2C).

SOST overexpression had no effect on bone properties in *Lrp5* WT or HBM mice when evaluated by three-point bending (Table S2).

II. A214V mice are more susceptible to the osteopenic effects of DKK1 overexpression than G171V mice

We next assessed the suppressive effects of DKK1 overexpression on bone properties in *Lrp5* WT and HBM mice. Consistent with previous reports of an osteopenic phenotype in these mice,[20] the $^{2.3kb}$*Col1a1-Dkk1* transgene significantly reduced whole body aBMD and BMC in *Lrp5* WT mice (Fig. 3A&B; Fig S2). DKK1 overexpression reduced aBMD by 7% in *Lrp5* WT males ($p=0.02$) and by 9% in WT females ($p<0.001$) (Fig. 3A&B). A similar magnitude effect of DKK1 overexpression was observed in *Lrp5* A214V mice (11% reduction in females and 14% reduction in males; $p<0.001$ for both sexes), and in female (7% reduction; $p=0.008$), but not male (0.2% reduction; p=0.94) *Lrp5* G171V mice.

In the distal femoral metaphysis, DKK1 overexpression in *Lrp5* WT mice reduced trabecular BV/TV by 58% and 38% in females and males, respectively ($p=0.006$ for females, $p=0.07$ for males; Fig. 3C). Femoral BV/TV was similarly suppressed by the *Dkk1* transgene in female and male *Lrp5* A214V mice (32% and 33%, $p=0.009$ and $p=0.004$ respectively), but not in either female or male G171V mice (Fig. 3C&E). Although the $^{2.3kb}$*Col1a1-Dkk1* transgene significantly reduced vertebral BV/TV in *Lrp5* WT mice, it did not in *Lrp5* HBM mice (Fig. 3D). Other μCT-derived parameters for femoral and vertebral trabecular structure affected A214V mice to a greater extent than G171V mice (Table S3).

When we measured bone formation rates, we did not observe consistent data in males and females for any *Lrp5* and *Dkk1* transgene group (Fig. 4A and Table S4). We also did not

detect *Dkk1*-induced differences in CtX values in *Lrp5* WT or HBM mice (Fig. 4B). Although the $^{2.3kb}$*Col1a1-Dkk1* transgene did not significantly reduce bone mechanical properties in *Lrp5* WT mice, it did reduce energy to ultimate force, ultimate force, and stiffness in male and female A214V mice and ultimate force and stiffness in female, but not male, G171V mice (Fig. 4C and Table S4).

III. A214V and G171V HBM receptors are expressed similarly in bone

Since *in vitro* studies of *Lrp5* HBM alleles involved overexpression of the receptors and their chaperones (e.g., MESD) in cultured cells, we examined the endogenous level of LRP5 receptor in protein extracts from diaphyseal bone and from liver in *Lrp5* WT, knockout, A214V, and G171V mice (Fig. 5). As expected, no immunodetectable protein was present in knockout mice. Two immunoreactive bands were detected in WT, A214V, and G171V mice, which likely represent post-translational modification by glycosylation.[27] We did not observe a consistent difference in the abundance of LRP5 receptor in protein extracts from WT and HBM mouse liver or bone. However, we were unable to reliably quantify cell surface receptor levels using techniques such as biotinylation (data not shown) and, consequently, could not determine whether there was a difference in the abundance of A214V and G171V receptor at the cell surface.

Discussion

This study addresses one mechanism by which *Lrp5* HBM-causing mutations affect bone properties, which is by making the LRP5 receptor less susceptible to antagonism by endogenous inhibitors. We tested this mechanism *in vivo* using mice with knock-in HBM alleles of *Lrp5* and with transgenes overexpressing the secreted inhibitors SOST and DKK1. We used two different promoters to drive expression of the secreted inhibitors. SOST is normally expressed by osteocytes; thus we used an osteocyte-specific promoter (^{8kb}*Dmp1*) to drive that transgene. In bone tissue, DKK1 is expressed more broadly—by osteocytes and osteoblasts; thus we used the osteoblast and osteocyte selective $^{2.3kb}$*Col1a1* promoter to drive that transgene. The different promoter strategy we used for these experiments had the advantage of more closely recapitulating the naturally occurring cell-specific expression profile. However, this strategy had the disadvantage of precluding direct comparisons between DKK1 and SOST overexpression. The ^{8kb}*Dmp1-SOST* mouse model exhibits a 1.3-fold increase in *SOST* transcript abundance and a 1.6-fold increase in total (murine + human) SOST protein in bone [21]. In contrast, the $^{2.3kb}$*Col1a1-Dkk1* mouse model exhibits a ~20-fold increase in *Dkk1* mRNA expression compared non-transgenic animals, though the effect on DKK1 protein abundance was not reported [20].

We confirmed that SOST overexpression reduced bone properties in *Lrp5* WT mice and found that it did not significantly reduce bone properties in either the *Lrp5* A214V or the G171V HBM mice. Several measures of bone formation and bone mass decreased non-significantly when SOST was overexpressed in *Lrp5* HBM mice, likely due to the inhibitory action of SOST on LRP6 which also affects bone mass in mice.[28] However, the bone properties in mice with *Lrp5* HBM alleles and SOST overexpression remained substantially

higher than those of WT mice, indicating that the effect of the HBM LRP5 receptor supersedes that of LRP6 in this context.

Similar, but not identical, results were obtained when DKK1 was overexpressed. DKK1 overexpression tended to reduce bone properties in *Lrp5* WT mice, but reached significance in males and females only for measures of aBMD, BMC, 5th lumbar vertebra BV/TV, and trabecular number in the distal femur and lumbar vertebra. In contrast to SOST overexpression, where *Lrp5* A214V and G171V mice were equally resistant, *Lrp5* A214V HBM mice were less resistant to the effects of DKK1 overexpression than G171V mice. For example, DKK1 overexpression in male and female *Lrp5* A214V mice caused significant reductions in aBMD, distal femur BV/TV, distal femur and vertebral body trabecular number, and ultimate force in 3-point bending tests, whereas no consistent reductions were observed in the *Lrp5* G171V mice. Even when DKK1 overexpression reduced bone properties in *Lrp5* HBM mice, the resultant bone properties were still substantially higher than those of WT mice. This observation suggests that substantial HBM LRP5 receptor signaling and bone mass accrual occur before the *Dkk1* transgene becomes expressed, or at sites or in cells that are less susceptible to DKK1 overexpression by osteoblasts and osteocytes.

Our *in vivo* data are consistent with *in vitro* studies that implicated decreased inhibition by SOST as the primary mechanism by which all known *Lrp5* HBM mutations produce increased bone mass, [29–31] and with our previous *in vivo* studies showing similarity between *Sost*$^{-/-}$ and *Lrp5* HBM mutant mouse model phenotypes.[32] The data also suggest that some HBM LRP5 receptor mutations can affect the sensitivity of the receptor to inhibition by DKK1, but this result is less certain. Various scenarios may account for the difference between *Lrp5* A214V and G171V mice in their response to DKK1 overexpression. First, DKK1 binds both the first and the third β-propeller of LRP5/6 [15, 19, 33], and consequently might be expected to only partially alter receptor function when missense mutations are introduced into the first β-propeller alone. Several studies have reported impaired DKK1 binding and/or DKK1-mediated inhibition of WNT signaling for the G171V and A214T HBM LRP5 mutants.[9, 10, 12, 34] However, others showed that DKK1 inhibits G171V and A214T similar to WT LRP5 when compared in parallel with mutations in the third beta propeller.[11, 19] However, all *in vitro* studies are limited in that the conditions used to assess DKK1 and LRP5 interaction may not have been physiologically relevant.[35] Our *in vivo* data suggest that under physiologic conditions DKK1 overexpression inhibits A214V differently than G171V.

Second, it has also been suggested that G171V mutant receptors do not traffic normally to the cell surface, leaving the receptor capable of transducing intracellular WNT signals while being resistant to extracellular DKK1 or SOST.[19] Again, since this mechanism was proposed based on *in vitro* overexpression experiments, the *in vivo* relevance is uncertain. We performed western blot analyses of LRP5 extracted from liver and cortical diaphyseal bone of *Lrp5* WT, knockout, A214V and G171V mice. It has previously been reported that LRP5/6 receptors within the secretory pathway migrate at ~180 kDa while receptor observed at the plasma membrane migrates more slowly at ~200 kDa [27]. The anti-LRP5 antibody we used did not detect LRP5 in knockout mice, indicating that the antibody is specific. We

observed immunodetectable LRP5 in bone and liver extracts from WT, A214V and G171V mice, but did not see any consistent differences between mice with the different genotypes. Importantly, each mouse had the larger molecular weight LRP5 band, likely representing receptor that has trafficked to the cell surface.[27] Although *in vitro* overexpression studies were able to identify cell-surface-localized LRP5 using biotinylation and immunoprecipitation,[27] we were unable to recover sufficient amounts of endogenous LRP5 following biotinylation and IP of membrane proteins from cultured embryonic fibroblasts to determine whether the amount of receptor at the surface differed between mice with A214V and G171V alleles.

Third, we cannot preclude the possibility that background differences between the A214V and G171V strains account for their differing response to DKK1 overexpression by influencing the level of *Dkk1* transgene expression and/or the relative contribution of LRP5 and LRP6 to bone anabolism. Backcrossing all strains onto the same genetic background would minimize the effect of this variable in future experiments.

When an effect of DKK1 overexpression was found in G171V mice, it was only in females. These results could represent false positives caused by multiple hypothesis testing, since many bone parameters were analyzed, or could suggest sex-specific effects of the transgene or the *Lrp5* allele. Sex-specific effects have been reported in mice harboring other mutations that affect WNT signaling. For example, female mice with osteocyte deletion (^{10kb}*Dmp1-Cre*-mediated) of *Ctnnb1* (which encodes *β-catenin*) are more severely affected than their male counterparts [36]. Further, 17 β-estradiol, but not testosterone, inhibits the increase in SOST that normally accompanies sex steroid deficiency [37]. It remains to be confirmed if and how *Lrp5* HBM mutations affect cross-talk between the WNT and sex-steroid signaling pathways.

In conclusion, mice with *Lrp5* A214V and G171V knock-in alleles are resistant to the osteopenic effects of SOST and DKK1 overexpression, although DKK1 overexpression does affect bone properties in A214V mice more than in G171V mice. These data provide *in vivo* support for the hypothesis that HBM mutations increase bone properties by reducing the endogenous inhibition of the LRP5 receptor. Still left to be determined is whether the resistance to inhibition of certain HBM-causing mutations is due to altered trafficking to the cell surface or altered binding to some endogenous inhibitors and not others. Studies that can precisely define the mechanism(s) of action for HBM-causing mutations have the potential to yield improved therapies for augmenting bone mass and preventing fractures.

Acknowledgements

This work was supported by NIH grants AR53237 (to AGR and MLW), AR060359 (to AGR and XH), and DK076007 (to TB), by the Howard Hughes Medical Institute (to MLW), and by VA grant I01BX001478 (to AGR). The *Dkk1* transgenic mice were kindly provided by Bill Richards and Amgen, Inc. PJN performed the in vivo experiments on DKK1/SOST overexpressing and *Lrp5* HBM mice, and co-wrote the initial draft of the paper; RK analyzed bone scans; MZ performed western blots from tissue lysates; BTM, TB, XH and MLW contributed to data interpretation and discussion; AGR designed the experiments and co-wrote the initial draft of the paper. All co-authors read and revised the manuscript and approved the final version. The authors thank Drs. V. Salazar and R. Civitelli for sharing unpublished data and their method for extracting LRP5 from cortical bone.

References

1. Baron R, Kneissel M. WNT signaling in bone homeostasis and disease: from human mutations to treatments. Nat Med. 2013; 19(2):179–192. [PubMed: 23389618]
2. Ai MR, Heeger S, Bartels CF, et al. Clinical and molecular findings in osteoporosis-pseudoglioma syndrome. American Journal of Human Genetics. 2005; 77(5):741–753. [PubMed: 16252235]
3. Gong Y, Slee RB, Fukai N, et al. LDL receptor-related protein 5 (LRP5) affects bone accrual and eye development. Cell. 2001; 107(4):513–523. [PubMed: 11719191]
4. Holmen SL, Giambernardi TA, Zylstra CR, et al. Decreased BMD and limb deformities in mice carrying mutations in both Lrp5 and Lrp6. J Bone Miner Res. 2004; 19(12):2033–2040. [PubMed: 15537447]
5. Kokubu C, Heinzmann U, Kokubu T, et al. Skeletal defects in ringelschwanz mutant mice reveal that Lrp6 is required for proper somitogenesis and osteogenesis. Development. 2004; 131(21): 5469–5480. [PubMed: 15469977]
6. Mani A, Radhakrishnan J, Wang H, et al. LRP6 mutation in a family with early coronary disease and metabolic risk factors. Science. 2007; 315(5816):1278–1282. [PubMed: 17332414]
7. Kubota T, Michigami T, Sakaguchi N, et al. Lrp6 hypomorphic mutation affects bone mass through bone resorption in mice and impairs interaction with Mesd. J Bone Miner Res. 2008; 23(10):1661–1671. [PubMed: 18505367]
8. Boyden LM, Mao JH, Belsky J, et al. High bone density due to a mutation in LDL-receptor-related protein 5. New England Journal of Medicine. 2002; 346(20):1513–1521. [PubMed: 12015390]
9. Bhat BM, Allen KM, Liu W, et al. Structure-based mutation analysis shows the importance of LRP5 beta-propeller 1 in modulating Dkk1-mediated inhibition of Wnt signaling. Gene. 2007; 391(1–2): 103–112. [PubMed: 17276019]
10. Ai M, Holmen SL, Van Hul W, et al. Reduced affinity to and inhibition by DKK1 form a common mechanism by which high bone mass-associated missense mutations in LRP5 affect canonical Wnt signaling. Mol Cell Biol. 2005; 25(12):4946–4955. [PubMed: 15923613]
11. Semenov MV, He X. LRP5 mutations linked to high bone mass diseases cause reduced LRP5 binding and inhibition by SOST. Journal of Biological Chemistry. 2006; 281(50):38276–38284. [PubMed: 17052975]
12. Ellies DL, Viviano B, McCarthy J, et al. Bone density ligand, sclerostin, directly interacts with LRP5 but not LRP5(G171V) to modulate Wnt activity. Journal of Bone and Mineral Research. 2006; 21(11):1738–1749. [PubMed: 17002572]
13. Bourhis E, Wang W, Tam C, et al. Wnt antagonists bind through a short peptide to the first beta-propeller domain of LRP5/6. Structure. 2011; 19(10):1433–1442. [PubMed: 21944579]
14. Binnerts ME, Tomasevic N, Bright JM, et al. The first propeller domain of LRP6 regulates sensitivity to DKK1. Mol Biol Cell. 2009; 20(15):3552–3560. [PubMed: 19477926]
15. Ahn VE, Chu ML, Choi HJ, et al. Structural Basis of Wnt Signaling Inhibition by Dickkopf Binding to LRP5/6. Dev Cell. 2011; 21(5):862–873. [PubMed: 22000856]
16. Cheng Z, Biechele T, Wei Z, et al. Crystal structures of the extracellular domain of LRP6 and its complex with DKK1. Nat Struct Mol Biol. 2011; 18(11):1204–1210. [PubMed: 21984209]
17. Mao J, Wang J, Liu B, et al. Low-density lipoprotein receptor-related protein-5 binds to Axin and regulates the canonical Wnt signaling pathway. Mol Cell. 2001; 7(4):801–809. [PubMed: 11336703]
18. Bao J, Zheng JJ, Wu D. The structural basis of DKK-mediated inhibition of Wnt/LRP signaling. Sci Signal. 2012; 5(224):pe22. [PubMed: 22589387]
19. Zhang Y, Wang Y, Li X, et al. The LRP5 high-bone-mass G171V mutation disrupts LRP5 interaction with Mesd. Mol Cell Biol. 2004; 24(11):4677–4684. [PubMed: 15143163]
20. Li J, Sarosi I, Cattley RC, et al. Dkk1-mediated inhibition of Wnt signaling in bone results in osteopenia. Bone. 2006; 39(4):754–766. [PubMed: 16730481]
21. Tu X, Rhee Y, Condon K, et al. Sost downregulation and local Wnt signaling are required for the osteogenic response to mechanical loading. Bone. 2011

22. Cui Y, Niziolek PJ, MacDonald BT, et al. Lrp5 functions in bone to regulate bone mass. Nat Med. 2011; 17(6):684–691. [PubMed: 21602802]
23. Sawakami K, Robling AG, Ai M, et al. The Wnt co-receptor LRP5 is essential for skeletal mechanotransduction but not for the anabolic bone response to parathyroid hormone treatment. J Biol Chem. 2006; 281(33):23698–23711. [PubMed: 16790443]
24. Atti E, Tetradis S, Magyar CE, et al. Thermoreversible Pluronic F108 Gel as a Universal Tissue Immobilization Material for Micro-Computed Tomography Analyses. J Bone and Miner Res. 2008; 23(S1):S362.
25. Bouxsein ML, Boyd SK, Christiansen BA, et al. Guidelines for assessment of bone microstructure in rodents using micro-computed tomography. J Bone Miner Res. 2010; 25(7):1468–1486. [PubMed: 20533309]
26. McAteer ME, Niziolek PJ, Ellis SN, et al. Mechanical stimulation and intermittent parathyroid hormone treatment induce disproportional osteogenic, geometric, and biomechanical effects in growing mouse bone. Calcif Tissue Int. 2010; 86(5):389–396. [PubMed: 20306026]
27. Hsieh JC, Lee L, Zhang L, et al. Mesd encodes an LRP5/6 chaperone essential for specification of mouse embryonic polarity. Cell. 2003; 112(3):355–367. [PubMed: 12581525]
28. Riddle RC, Diegel CR, Leslie JM, et al. Lrp5 and Lrp6 exert overlapping functions in osteoblasts during postnatal bone acquisition. PLoS One. 2013; 8(5):e63323. [PubMed: 23675479]
29. Li X, Zhang Y, Kang H, et al. Sclerostin binds to LRP5/6 and antagonizes canonical Wnt signaling. J Biol Chem. 2005; 280(20):19883–19887. [PubMed: 15778503]
30. Semenov M, Tamai K, He X. SOST is a ligand for LRP5/LRP6 and a Wnt signaling inhibitor. J Biol Chem. 2005; 280(29):26770–26775. [PubMed: 15908424]
31. van Dinther M, Zhang J, Weidauer SE, et al. Anti-Sclerostin antibody inhibits internalization of Sclerostin and Sclerostin-mediated antagonism of Wnt/LRP6 signaling. PLoS One. 2013; 8(4):e62295. [PubMed: 23638027]
32. Niziolek PJ, Farmer TL, Cui Y, et al. High-bone-mass-producing mutations in the Wnt signaling pathway result in distinct skeletal phenotypes. Bone. 2011; 49(5):1010–1019. [PubMed: 21855668]
33. Chen S, Bubeck D, Macdonald BT, et al. Structural and Functional Studies of LRP6 Ectodomain Reveal a Platform for Wnt Signaling. Dev Cell. 2011; 21(5):848–861. [PubMed: 22000855]
34. Balemans W, Piters E, Cleiren E, et al. The Binding Between Sclerostin and LRP5 is Altered by DKK1 and by High-Bone Mass LRP5 Mutations. Calcif Tissue Int. 2008
35. Goel S, Chin EN, Fakhraldeen SA, et al. Both LRP5 and LRP6 receptors are required to respond to physiological Wnt ligands in mammary epithelial cells and fibroblasts. J Biol Chem. 2012; 287(20):16454–16466. [PubMed: 22433869]
36. Kramer I, Halleux C, Keller H, et al. Osteocyte Wnt/beta-catenin signaling is required for normal bone homeostasis. Mol Cell Biol. 2010; 30(12):3071–3085. [PubMed: 20404086]
37. Modder UI, Clowes JA, Hoey K, et al. Regulation of circulating sclerostin levels by sex steroids in women and in men. J Bone Miner Res. 2011; 26(1):27–34. [PubMed: 20499362]

Significance Statement

The mechanism of action for High Bone Mass (HBM)-causing mutations in the LRP5 receptor have been postulated to occur via reduced inhibition by secreted LRP5/6 antagonists, based on cell culture overexpression models. Anti-sclerostin and anti-DKK1 antibody therapies are being developed to build bone and prevent fractures among individuals with various diseases of low bone mass, most notably osteoporosis. Here we show in an *in vivo* model that sclerostin overexpression fails to manifest its osteopenic effects in two *Lrp5* HBM knock-in mouse mutants – G171V and A214V. However, DKK1 overexpression has osteopenic effects in A214V but not G171V mutant mice. The data highlight the existence of multiple mechanisms of action for HBM-causing alleles of *Lrp5*, in an *in vivo* context.

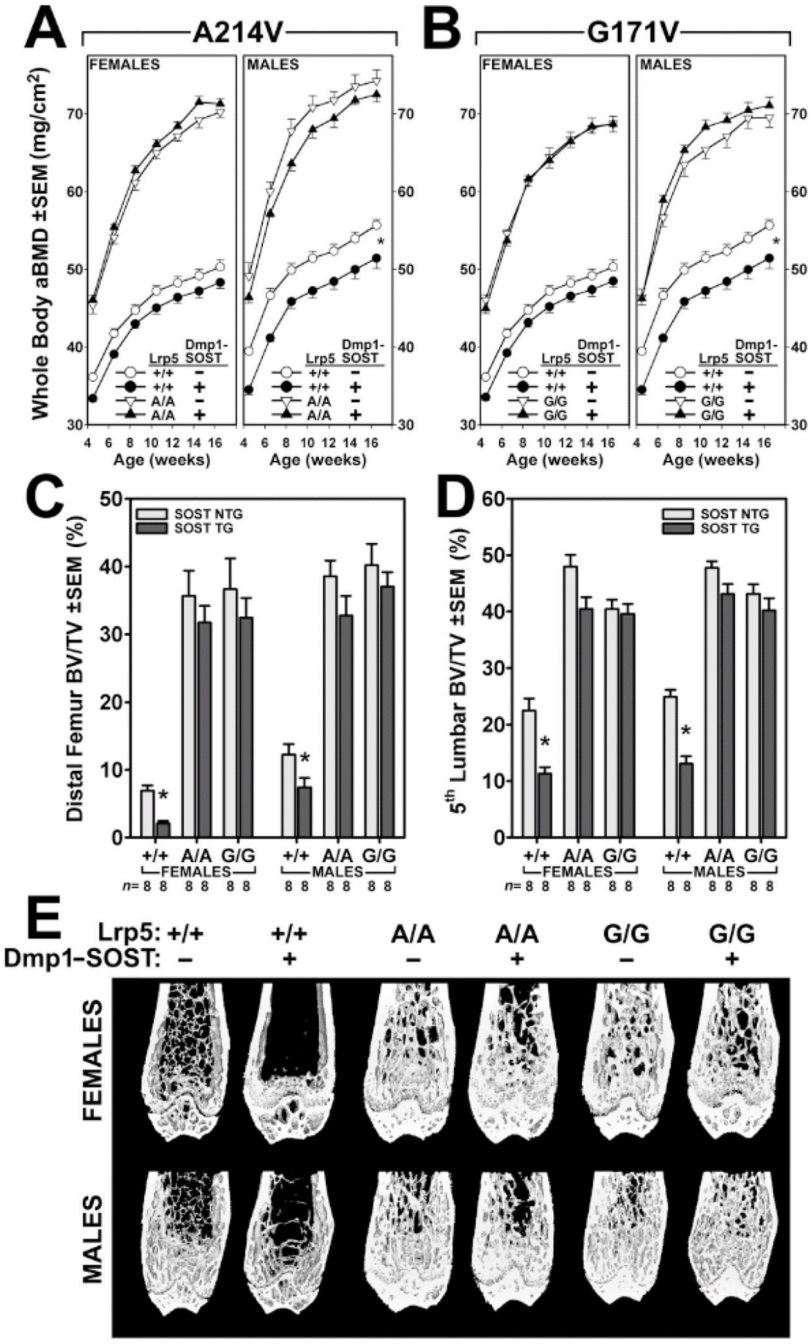

Figure 1.

Whole body areal bone mineral density (aBMD) measured every 2 wks, beginning at 4.5 wks of age and ending at 16.5 wks of age, in (**A**) *Lrp5* A214V mutant mice (A/A), and in (**B**) *Lrp5* G171V mutant mice (G/G), with (+) or without (-) the ^{8kb}*Dmp1-SOST* transgene. *p<0.05 from a repeated measures ANOVA for the *SOST* transgene main effect within *Lrp5* genotype. Trabecular bone volume fraction (BV/TV) in (**C**) the distal femoral metaphysis and (**D**) the fifth lumbar vertebra, from 17-wk-old male and female *Lrp5* +/+, A/A, and G/G mice, with (TG) or without (NTG) the ^{8kb}*Dmp1-SOST* transgene. *p<0.05 NTG vs TG

within same *Lrp5*/sex group. Additional μCT parameters are reported in supplemental Table S1. (**E**) Representative cut-away μCT images of the distal femur from the groups indicated in panel **C**. Note the reduced trabecular bone mass induced by the *SOST* transgene and the increase in bone mass induced by the *Lrp5* HBM alleles. *Lrp5* WT data are repeated across graphs within panels A and B (for each sex) for clarity of the *Lrp5* HBM curves. Sample sizes for the DEXA data (**A** and **B**) and the μCT data (**C** and **D**) are *n*=8/group.

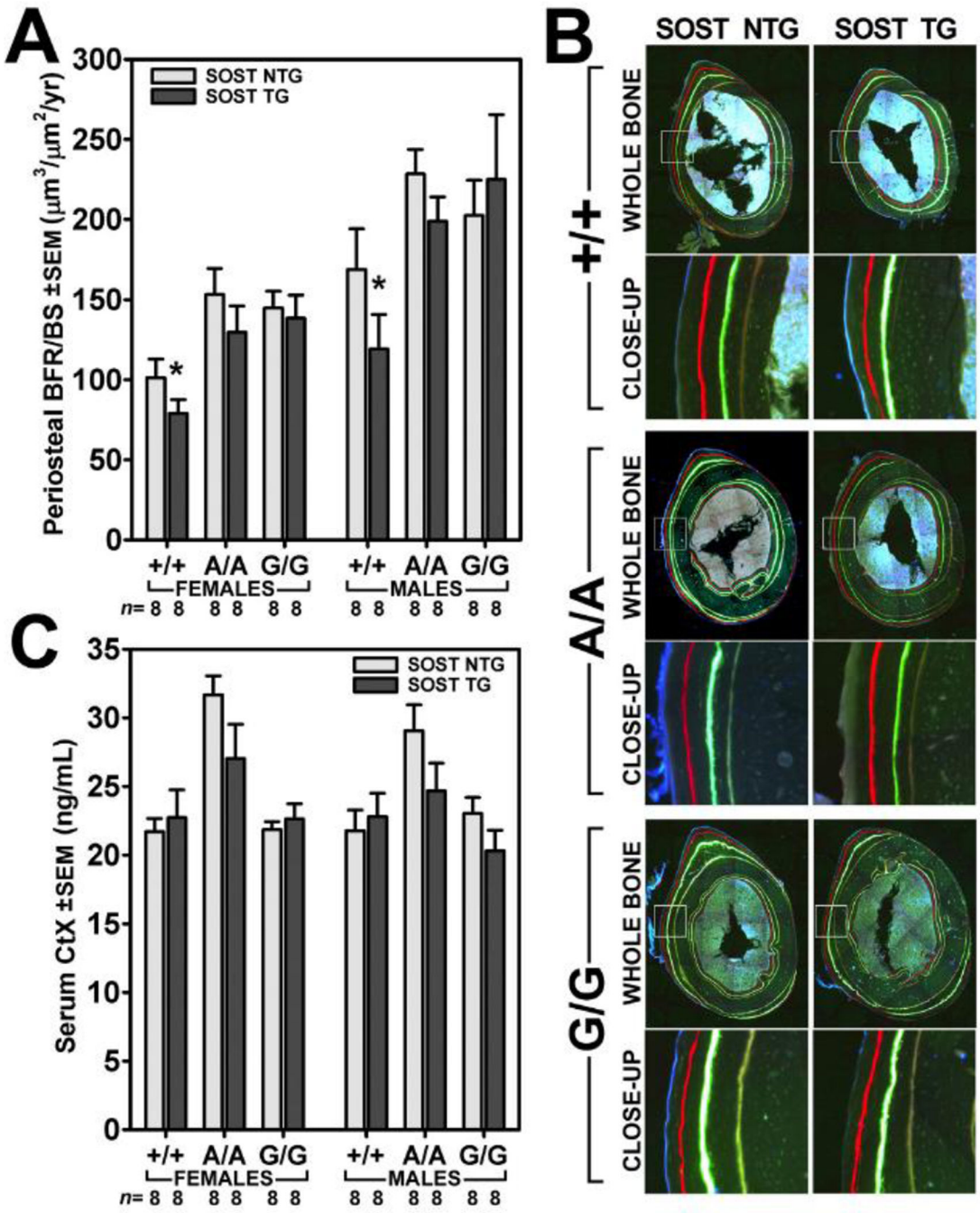

Figure 2.

Bone formation and resorption indices male and female *Lrp5* WT (+/+), *Lrp5* A214V homozygous knock-in (A/A), and *Lrp5* G171V homozygous knock-in (G/G) mice, with (+) or without (−) the ^{8kb}*Dmp1-SOST* transgene. (**A**) Periosteal bone formation rate per unit bone surface (BFR/BS) was measured over the post-weaning growth phase of the mice using an oxytetracycline label administered at 5 wks and an alizarin complexone label administered at 12 wks. (**B**) Whole bone and close-up photomicrographs of the fluorochrome labeling (male mice are shown) from the experimental groups showing

periosteal bone formation. The central label is a calcein label administered at 8 wks, which was not used for the measurements shown in panel **A**. Histomorphometric measurements using this label as the first label, rather than the tetracycline label, produced nearly identical results as those generated using the tetracycline label (data not shown). (**C**) Serum collected at 7 wks of age was assayed for the resorption marker carboxy-terminal collagen crosslinks (CtX). *=$p<0.05$ TG vs NTG within same *Lrp5*/sex group. Additional histomorphometric parameters are reported in supplemental Table S2. Sample sizes are indicated along the x-axis.

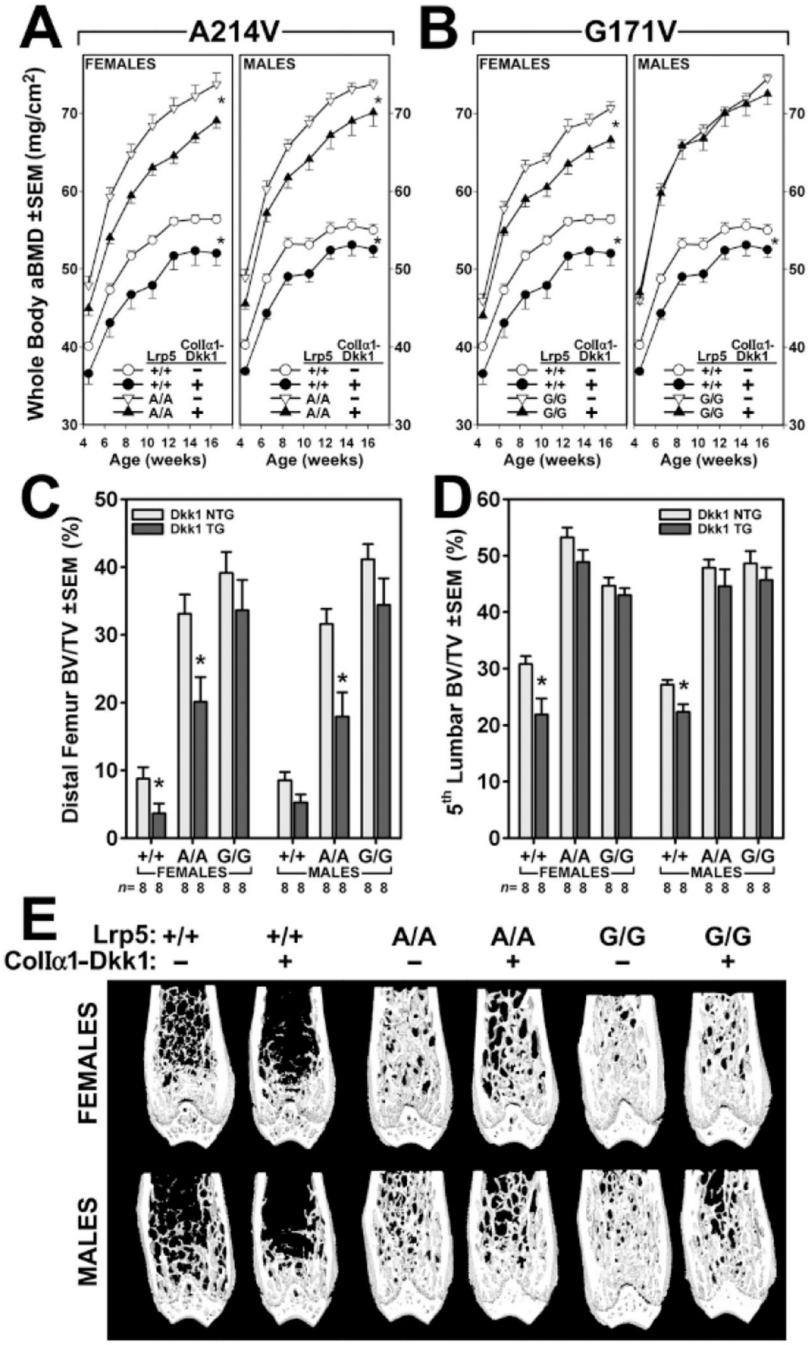

Figure 3.

Whole body areal bone mineral density (aBMD) measured every 2 wks, beginning at 4.5 wks of age and ending at 16.5 wks of age, in (**A**) *Lrp5* A214V mutant mice (A/A), and in (**B**) *Lrp5* G171V mutant mice (G/G), with (+) or without (−) the $^{2.3kb}$*Col1a1-Dkk1* transgene. *p<0.05 from a repeated measures ANOVA for the *Dkk1* transgene main effect within *Lrp5* genotype. Trabecular bone volume fraction (BV/TV) in (**C**) the distal femoral metaphysis and (**D**) the fifth lumbar vertebra, from 17-wk-old male and female *Lrp5* +/+, A/A, and G/G mice, with (TG) or without (NTG) the $^{2.3kb}$*Col1a1-Dkk1* transgene. *p<0.05

NTG vs TG within same *Lrp5*/sex group. Additional μCT parameters are reported in supplemental Table S3. (**E**) Representative cut-away μCT images of the distal femur from the groups indicated in panel **C**. Note the reduced trabecular bone mass induced by the *Dkk1* transgene and the increase in bone mass induced by the *Lrp5* HBM alleles. *Lrp5* WT data are repeated across graphs within panels A and B (for each sex) for clarity of the *Lrp5* HBM curves. Sample sizes for the DEXA data (**A** and **B**) and the μCT data (**C** and **D**) are *n*=8/group.

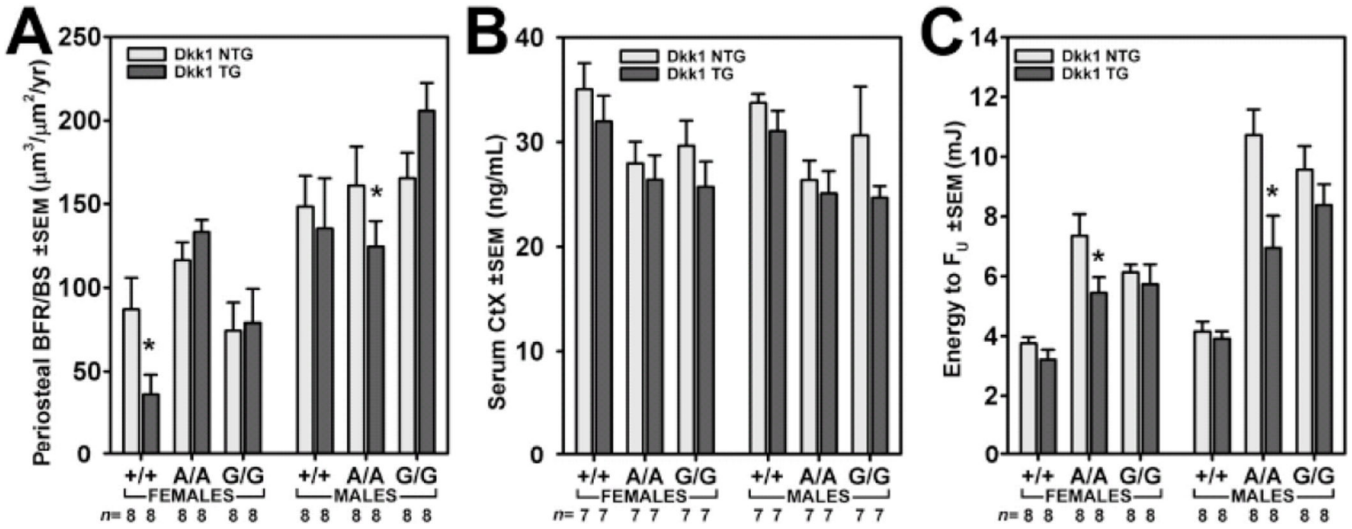

Figure 4.

Periosteal bone formation rates, serum resorption indices, and whole bone mechanical properties in male and female *Lrp5* WT (+/+), *Lrp5* A214V homozygous knock-in (A/A), and *Lrp5* G171V homozygous knock-in (G/G) mice, with (+) or without (−) the $^{2.3kb}$*Col1a1-Dkk1*. (**A**) Periosteal bone formation rate per unit bone surface (BFR/BS) was measured over the post-weaning growth phase of the mice using an oxytetracycline label administered at 5 wks and an alizarin complexone label administered at 12 wks. (**B**) Serum collected at 7 wks of age was assayed for the resorption marker carboxy-terminal collagen crosslinks (CtX). (**C**) Energy to ultimate force derived from monotonic three-point bending tests to failure of femora from 17-wk-old male and female mice. *=p<0.05 TG vs NTG within same *Lrp5*/sex group. Sample sizes are indicated along the x-axis. Additional histomorphometric and biomechanical properties are reported in supplemental Table S4.

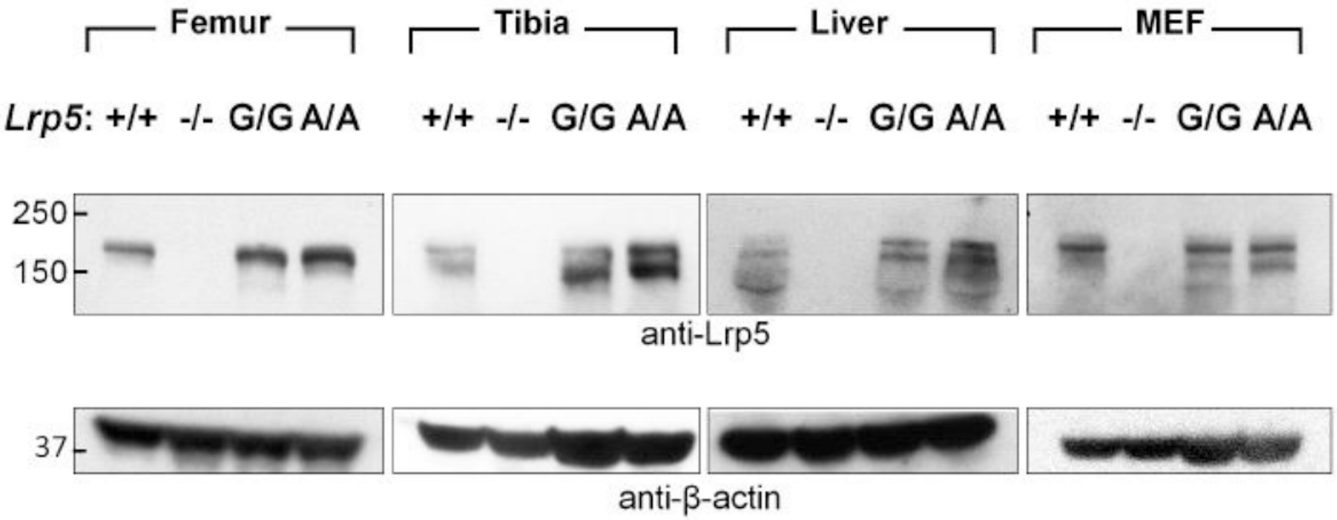

Figure 5.

Immunodetection of endogenous LRP5 from wild-type, knockout, and HBM mice. Protein lysates recovered from diaphyseal cortical bones, liver, or cultured mouse embryonic fibroblasts (MEF) were separated by SDS-PAGE on 4 – 12% gradient gels, transferred to PVDF, and immunodetected with an anti-LRP5 antibody followed by an anti-βactin antibody, as a loading control. Note the absence of immunoreactive bands in the *Lrp5* knockout (−/−) mice. Comparable amounts of immunodetectable LRP5 in WT (+/+) and HBM (G/G and A/A) mice are present in bones from different mice with each genotype (left of center panels); the same was found for LRP5 from liver and MEFs (right of center panels). At present, we do not know whether the two immunoreactive LRP5 bands seen in some blots represent the receptor's post-translational modification during its trafficking to the cell surface,[27] its different post-translational modifications tissues with multiple cell types, or its partial degradation during extraction.